View Online

NJC

New Journal of Chemistry

An international journal of the chemical sciences

www.rsc.org/njc

Volume 34 | Number 2 | February 2010 | Pages 173–368

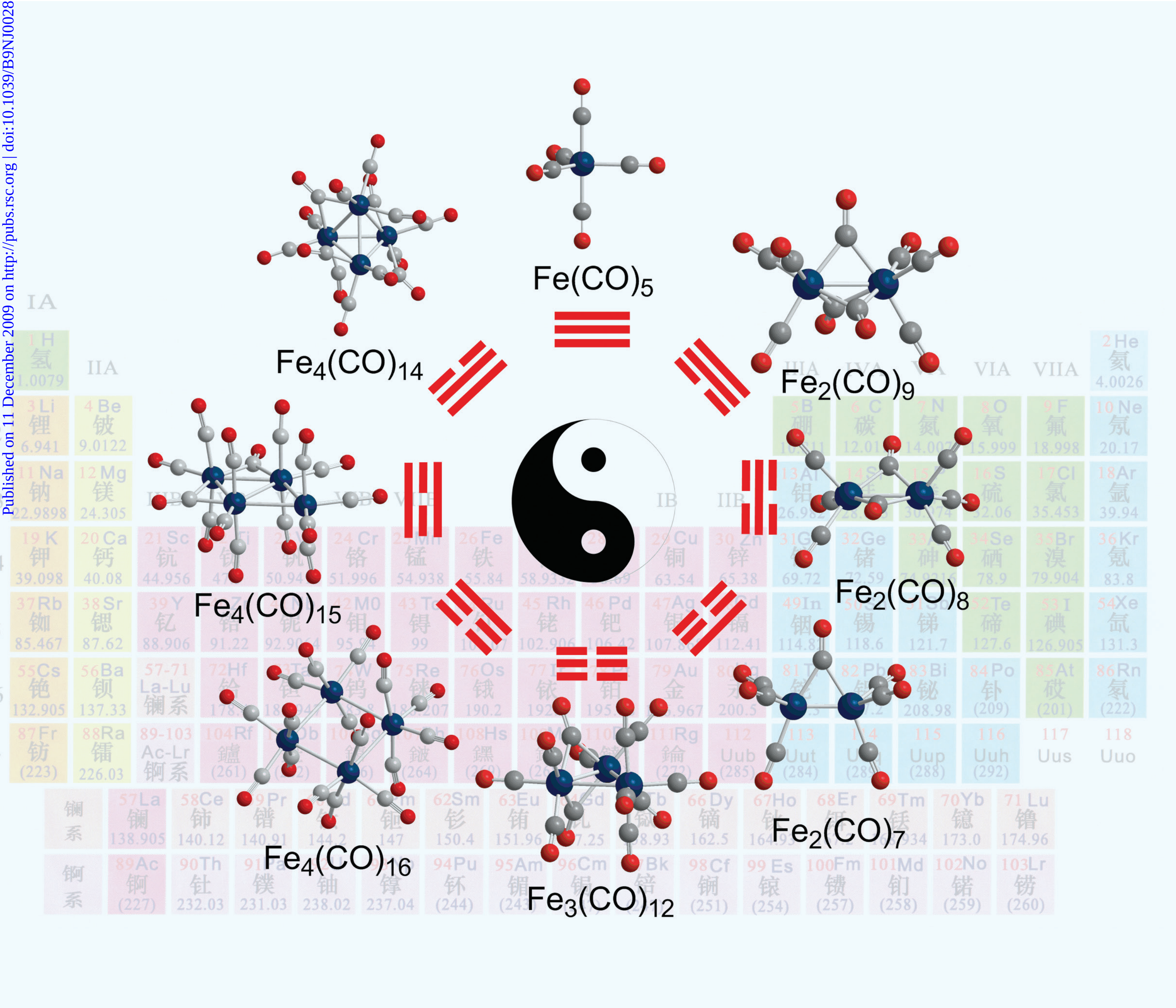

ISSN 1144-0546

RSC Publishing

PAPER

Qian-Shu Li and R. Bruce King *et al.*

Neutral homoleptic tetranuclear iron carbonyls: why haven't they been synthesized as stable molecules?

Neutral homoleptic tetranuclear iron carbonyls: why haven't they been synthesized as stable molecules?†

Ting Ting Shi,[a] Qian-Shu Li,*[ab] Yaoming Xie,[c] R. Bruce King*[ac] and
Henry F. Schaefer III[c]

Received (in Gainesville, FL, USA) 24th June 2009, Accepted 22nd October 2009
First published as an Advance Article on the web 11th December 2009
DOI: 10.1039/b9nj00284g

The tetranuclear iron carbonyls $Fe_4(CO)_n$ (n = 16, 15, 14) have been investigated using density functional theory (DFT). Low-energy structures are predicted for $Fe_4(CO)_{16}$, $Fe_4(CO)_{15}$, and $Fe_4(CO)_{14}$ in which the Fe_4 units are rhombi, planar butterflies, and tetrahedra with four, five, and six Fe–Fe single bonds, respectively, to give all four iron atoms the favored 18-electron configuration. However, for $Fe_4(CO)_{14}$ an alternative low energy structure is predicted with a planar Fe_4 butterfly and one of the five iron–iron distances short enough to correspond to a formal Fe=Fe double bond, thereby also leading to the favored 18-electron configuration. The dissociation energy of $Fe_4(CO)_{16}$ into $Fe(CO)_5$ + $Fe_3(CO)_{11}$ or $Fe_3(CO)_{12}$ + $Fe(CO)_4$ is predicted to be very low (<6 kcal mol^{-1}). Similarly, the dissociation energy of $Fe_4(CO)_{15}$ into $Fe(CO)_5$ + $Fe_3(CO)_{10}$ is predicted to be very low at ~ 5 kcal mol^{-1}. These low predicted dissociation energies of $Fe_4(CO)_{16}$ and $Fe_4(CO)_{15}$ into smaller iron carbonyl fragments are consistent with the fact that neither of these molecules have been synthesized or detected spectroscopically, even in low temperature matrices. However, $Fe_4(CO)_{14}$ is predicted to be considerably more stable towards dissociation into smaller fragments with a dissociation energy of 23.2 kcal mol^{-1} (B3LYP) or 39.2 kcal mol^{-1} (BP86) into $Fe(CO)_5$ + $Fe_3(CO)_9$. This is consistent with the detection of $Fe_4(CO)_{14}$ by infrared spectroscopy in the reaction product of mass selected Fe_4^+ with CO in low temperature matrices.

1. Introduction

The three simple homoleptic iron carbonyls $Fe(CO)_5$, $Fe_2(CO)_9$, and $Fe_3(CO)_{12}$ are stable enough for structural characterization by X-ray diffraction and are well-known commercially available reagents for synthetic organoiron chemistry and other applications. However, no stable neutral homoleptic tetranuclear carbonyls of iron, *i.e.*, $Fe_4(CO)_n$, are known even though its heavier congener osmium forms the three binary tetranuclear carbonyls $Os_4(CO)_n$ (n = 16, 15, 14). These tetranuclear osmium carbonyls provide examples of three different structural arrangements of the central Os_4 unit (Fig. 1). Thus $Os_4(CO)_{16}$ has a rhombus structure with four Os–Os single bonds,[1,2] $Os_4(CO)_{15}$ has a "butterfly" structure with five Os–Os single bonds,[3] and $Os_4(CO)_{14}$ has a tetrahedral structure with six Os–Os single bonds.[4] Both $Os_4(CO)_{15}$ and $Os_4(CO)_{14}$ appear to be very stable. However, $Os_4(CO)_{16}$, although stable enough for a low-temperature structural determination by X-ray diffraction, decomposes around room temperature to give mainly $Os_3(CO)_{12}$. Note that the total of 20 for the sum of the numbers of carbonyl groups and Os–Os single bonds in all three $Os_4(CO)_n$ structures (n = 16, 15, 14) corresponds to the favored 18-electron configuration for all four osmium atoms.

Despite the absence of any stable homoleptic tetranuclear iron carbonyls, there is some mass spectrometric evidence[5] for the existence of neutral $Fe_4(CO)_{14}$ in low-temperature matrices. Thus the codeposition of mass-selected Fe_4^+ with carbon monoxide at 25 K followed by neutralization of the resulting ions with an electron beam gives a pattern of ν(CO) frequencies that have been assigned to neutral $Fe_4(CO)_{14}$. This product appears to be stable only at very low temperatures and decomposes under ambient conditions. In addition, the tetranuclear iron carbonyl anion $Fe_4(CO)_{13}^{2-}$ has been known since 1930[6] but was characterized structurally only much later.[7] It is particularly interesting that although $Fe_4(CO)_{13}^{2-}$ has been known for nearly 80 years, no way of

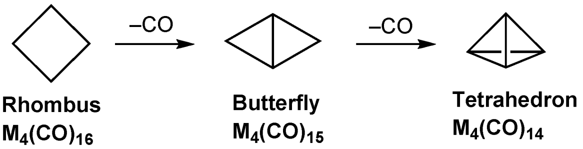

Fig. 1 Structures of tetranuclear metal carbonyls. The osmium derivatives (M = Os) are known and stable enough for structure determinations by X-ray diffraction.

---

[a] *Center for Computational Quantum Chemistry, South China Normal University, Guangzhou, 510631, China*
[b] *Institute of Chemical Physics, Beijing Institute of Technology, Beijing 100081, China*
[c] *Department of Chemistry and Center for Computational Chemistry, University of Georgia, Athens, Georgia 30602, USA. E-mail: rbking@chem.uga.edu, qsli@scnu.edu.cn*

† Electronic supplementary information (ESI) available: Tables S1 to S9: Cartesian coordinates for the nine optimized $Fe_4(CO)_n$ (n = 16, 15, 14) structures; Tables S10 to S18: harmonic vibrational frequencies for the nine optimized $Fe_4(CO)_n$ (n = 16, 15, 14) structures; complete Gaussian reference (ref. 27). See DOI: 10.1039/b9nj00284g

converting it to a stable neutral $Fe_4(CO)_n$ derivative has yet been found.

Theoretical work on the aromaticity of the Fe_4 skeletons in the $Fe_4(CO)_n$ (n = 16, 15, 14) was recently reported[8] using the nucleus independent chemical shifts (NICS) method to evaluate the aromaticity of the Fe_4 skeletons in structures analogous to the known osmium carbonyl derivatives. However, in that study no attempt was made to search comprehensively for all low energy $Fe_4(CO)_n$ (n = 16, 15, 14) structures.

The general objective of the research discussed in this paper is to elucidate the reason for the lack of stable neutral homoleptic tetranuclear iron carbonyls using density functional theory (DFT) methods. This research has the following more specific aims:

(1) Comparison of the predicted structures for $Fe_4(CO)_n$ (n = 16, 15, 14) with those predicted for the osmium analogues in a previous DFT study.[9]

(2) Elucidation of the thermodynamics for the dissociation of the lowest energy optimized $Fe_4(CO)_n$ structures into smaller fragments.

2. Theoretical methods

Density functional theory (DFT) methods have been acknowledged to be a practical and effective computational tool, especially for organometallic compounds.[10–18] Two density functional theory methods were used in this study, namely the B3LYP and BP86 methods. The B3LYP method is an HF/DFT hybrid method using Becke's three-parameter functional (B3)[19] and the Lee-Yang-Parr generalized gradient correlation functional (LYP).[20] The BP86 method is a pure DFT method, which combines Becke's 1988 exchange functional (B)[21] with Perdew's 1986 gradient correlation functional (P86).[22]

All-electron double zeta plus polarization (DZP) basis sets were used in this work. The DZP basis sets for C and O, which are designated (9s5p1d/4s2p1d), begin with Dunning's standard double zeta contraction[23] of Huzinaga's primitive sets (DZ)[24] and add one set of pure spherical harmonic d functions with orbital exponents $\alpha_d(C) = 0.75$ and $\alpha_d(O) = 0.85$. The loosely contracted DZP basis set for iron is the Wachters' primitive set[25] augmented by two sets of p functions and one set of d functions and contracted following Hood, Pitzer, and Schaefer,[26] designated as (14s11p6d/10s8p3d). With these basis sets the total numbers of the basis set functions are 676, 646, and 616 for $Fe_4(CO)_{16}$, $Fe_4(CO)_{15}$ and $Fe_4(CO)_{14}$, respectively.

The geometries of all of the structures were fully optimized using the DZP B3LYP and DZP BP86 methods. The vibrational frequencies were determined by evaluating analytically the second derivatives of the energy with respect to the nuclear coordinates. All of the computations were carried out with the Gaussian 03 program[27] in which the fine grid (75, 302) is the default for evaluating integrals numerically, and the tight designation is the default for the SCF convergence. To ensure computational precision, the tight convergence threshold (10^{-8} hartree) was used for the self-consistent field (SCF) procedure and the geometry optimization.

The optimized geometries from the B3LYP/DZP and BP86/DZP computations for the $Fe_4(CO)_n$ structures (n = 16, 15, 14) are depicted in Fig. 2, Fig. 3 and Fig. 4. In these figures the upper numbers are the predicted distances obtained by the B3LYP method whereas the lower numbers are the predicted distances obtained by the BP86 method. Table 1, Table 3 and Table 5 list the electronic states and energies and Table 2, Table 4 and Table 6 list the ν(CO) frequencies for the $Fe_4(CO)_n$ structures (n = 16, 15, 14).

3. Results and discussion

3.1 $Fe_4(CO)_{16}$

Four low-lying (within 7 kcal mol^{-1}) $Fe_4(CO)_{16}$ structures have been found (Fig. 2 and Table 1). The global minimum for $Fe_4(CO)_{16}$ predicted from our DFT studies is a D_4 square planar structure (**16-1** in Fig. 2, Table 1 and Table 2), with four terminal carbonyls attached to each iron atom. The corresponding $Os_4(CO)_{16}$ global minimum has lower symmetry (D_2) with the corresponding D_4 structure lying only about 1 kcal mol^{-1} higher in energy. The Fe–Fe distances in **16-1** are predicted to be 2.928 Å (B3LYP) or 2.868 Å (BP86) corresponding to the single bonds required to give each iron atom in $Fe_4(CO)_{16}$ the favored 18-electron configuration. This Fe–Fe distance is longer than those in the global minimum[28,29] for $Fe_3(CO)_{12}$ (2.59 to 2.74 Å with B3LYP or 2.57 to 2.71 Å with BP86) as well as the Fe–Fe distance predicted for the $Fe_3(CO)_{12}$ structure with all terminal carbonyls.[30]

The second lowest energy structure for $Fe_4(CO)_{16}$ is a D_{2d} rhombus structure with a non-planar central Fe_4 unit (**16-2** in Fig. 2, Table 1 and Table 2). Structure **16-2** lies 2.0 kcal mol^{-1} (B3LYP) or 4.6 kcal mol^{-1} (BP86) in energy above the global minimum **16-1** and has a very small imaginary vibrational frequency at 16i cm^{-1} (B3LYP) or at 18i cm^{-1} (BP86). The Fe–Fe distances are predicted to be 2.970 Å (B3LYP) or 2.921 Å (BP86) corresponding to the single bonds required to give each iron atom the favored 18-electron configuration.

The $Fe_4(CO)_{16}$ structure **16-3**, lying 4.3 kcal mol^{-1} (B3LYP) or 4.5 kcal mol^{-1} (BP86) above the global minimum **16-1**, is a genuine minimum with all real vibrational frequencies by both DFT methods. Structure **16-3** has two semibridging carbonyls and does not correspond to any of the structures previously predicted[9] for $Os_4(CO)_{16}$. The semibridging carbonyl groups in **16-3** are predicted to exhibit ν(CO) frequencies at 1824 and 1828 cm^{-1} (Table 2), which are significantly below the terminal ν(CO) frequencies found in **16-3** as well as the other $Fe_4(CO)_{16}$ structures. The butterfly-shaped Fe_4 skeleton of **16-3** consists of two triangles sharing an edge. The Fe–Fe distances bridged by CO groups in **16-3** are 2.936 Å (B3LYP) or 2.893 Å (BP86), while the unbridged Fe–Fe distances are longer at 3.133 Å (B3LYP) or 3.096 Å (BP86). The diagonal Fe–Fe distances are predicted to be 2.953 Å (B3LYP) or 2.867 Å (BP86). The Fe–C distances to the semibridging CO groups are 1.867 Å (B3LYP) or 1.868 Å (BP86) and 2.129 Å (B3LYP) or 2.126 Å (BP86).

The remaining structure predicted for $Fe_4(CO)_{16}$, namely **16-4** lying at 4.6 kcal mol^{-1} (B3LYP) or 7.2 kcal mol^{-1} (BP86)

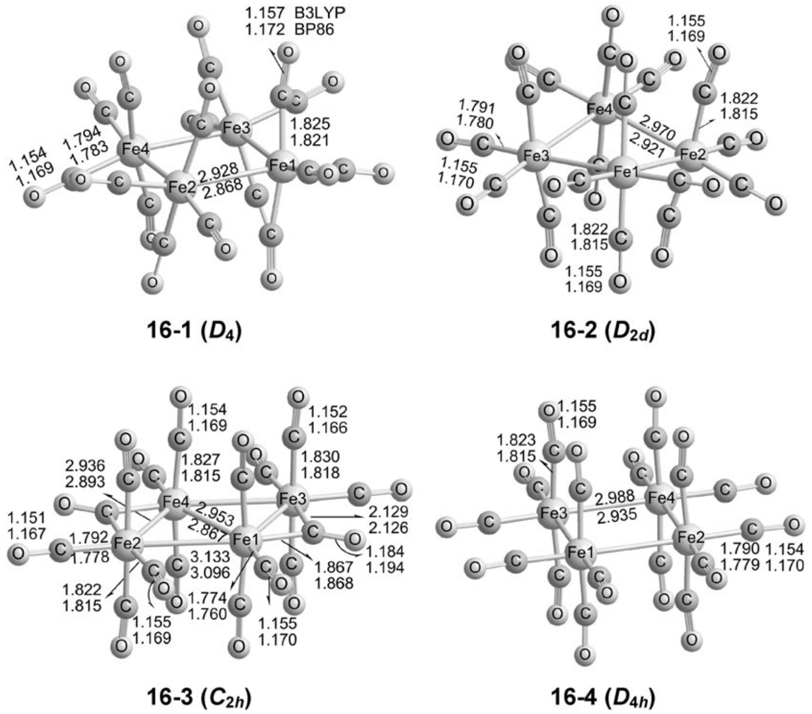

16-1 (D_4) 16-2 (D_{2d})

16-3 (C_{2h}) 16-4 (D_{4h})

Fig. 2 The four optimized structures of $Fe_4(CO)_{16}$. In Fig. 2, Fig. 3 and Fig. 4 the upper figures are the predicted distances obtained by the B3LYP method whereas the lower figures are the predicted distances obtained by the BP86 method.

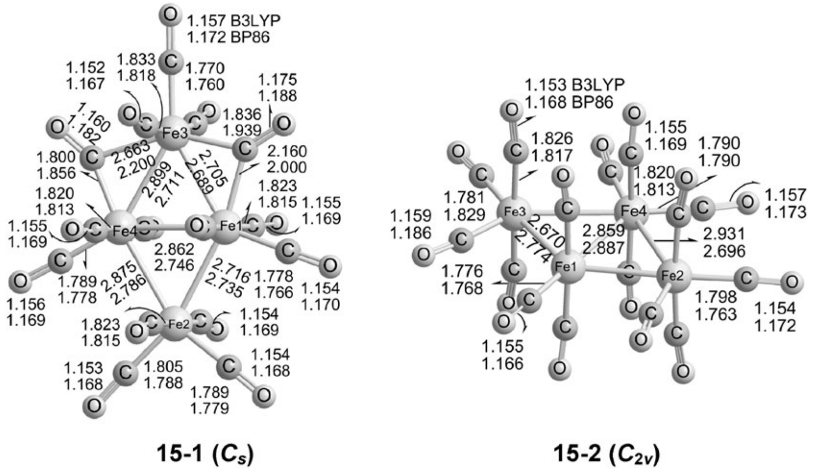

15-1 (C_s) 15-2 (C_{2v})

Fig. 3 The two optimized structures of $Fe_4(CO)_{15}$.

above **16-1**, has a square skeleton with D_{4h} symmetry. Structure **16-4** is a saddle point with two small imaginary vibrational frequencies. Following the corresponding normal modes (b_{2u} and a_{1u}) leads to either structure **16-1** or structure **16-2**, respectively.

3.2 $Fe_4(CO)_{15}$

Only two low-lying singlet structures for $Fe_4(CO)_{15}$ are found in the present work (Fig. 3, Table 3 and Table 4). Both of these structures have a planar Fe_4 butterfly framework. They differ by the arrangement of the carbonyl groups. No low-energy structures with a non-planar Fe_4 butterfly framework are predicted for $Fe_4(CO)_{15}$ in contrast to the previous DFT study[9] of $Os_4(CO)_{15}$ where a low-energy structure with a non-planar Os_4 butterfly was found.

The global minimum of $Fe_4(CO)_{15}$ is predicted to be the C_s structure **15-1** with a planar butterfly-shaped Fe_4 skeleton having one bridging and one semibridging carbonyl group (Fig. 3). The osmium analogue was previously predicted to have only the bridging carbonyl group with the remaining 14 carbonyl groups in terminal positions.[9] Structure **15-1** for $Fe_4(CO)_{15}$ can be derived from structure **16-3** for $Fe_4(CO)_{16}$ by removal of one of the bridging carbonyls and then converting one of the terminal carbonyl groups into a semibridging carbonyl group. These semibridging carbonyl groups in **15-1** are predicted to exhibit ν(CO) frequencies at 1854 and 1896 cm^{-1}, which are significantly higher than those in **16-3**.

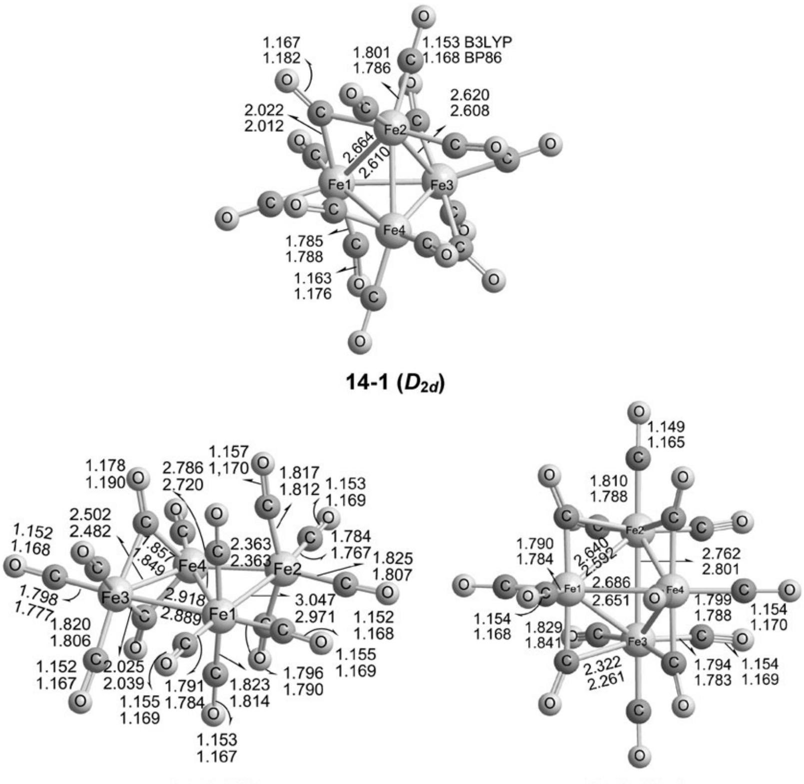

14-1 (D_{2d})

14-2 (C_s)

14-3 (C_{2v})

Fig. 4 The three optimized structures of $Fe_4(CO)_{14}$.

Table 1 The total energies (*E*, in Hartree), relative energies (Δ*E*, in kcal mol^{-1}), the zero-point corrected relative energies (Δ*E*(ZPE), in kcal mol^{-1}), and the numbers of imaginary vibrational frequencies (Nimag) for the structures of $Fe_4(CO)_{16}$

	16-1 (D_4)		**16-2** (D_{2d})		**16-3** (C_{2h})		**16-4** (D_{4h})	
Method	B3LYP	BP86	B3LYP	BP86	B3LYP	BP86	B3LYP	BP86
−*E*	6868.84271	6869.87083	6868.83976	6869.86352	6868.83594	6869.86376	6868.83546	6869.85950
Δ*E*	0	0	2.0	4.6	4.3	4.5	4.6	7.2
Δ*E*(ZPE)	0	0	2.3	5.0	4.3	4.5	5.2	7.8
Nimag	0	0	1 (16*i*)	1 (18*i*)	0	0	2 (23*i*,19*i*)	2(24*i*,22*i*)

Table 2 The infrared n(CO) vibrational frequencies (cm^{-1}) predicted for the four $Fe_4(CO)_{16}$ structures (infrared intensities in parentheses are in km mol^{-1}, bridging ν(CO) frequencies in **bold**)

16-1	1942(0), 1960(21), 1960(21), 1961(0), 1977(18), 1979(74), 1979(74), 1991(9) 1991(9), 2001(2870), 2002(0), 2004(0), 2012(0), 2038(2631), 2038(2631), 2081(0)
16-2	1961(0), 1971(27), 1971(27), 1971(0), 1979(80), 1982(76), 1982(76), 1993(78) 1993(78), 2004(0), 2007(168), 2017(0), 2020(2500), 2038(2621), 2038(2621), 2086(0)
16-3	**1824(691)**, **1828(0)**, 1961(0), 1966(45), 1980(2), 1981(0), 1990(184), 1996(0) 1999(0), 2014(346), 2017(0), 2022(2761), 2025(2294), 2028(0), 2052(2470), 2090(0)
16-4	1955(0), 1971(0), 1972(0), 1976(0), 1976(0), 1980(21), 1980(21), 1994(126) 1994(126), 2005(0), 2008(0), 2016(2765), 2018(0), 2039(2671), 2039(2671), 2085(0)

The Fe–Fe distances in **15-1** are all shorter than those in **16-3**. Thus the diagonal Fe–Fe distance in **15-1** (2.862 Å by B3LYP or 2.746 Å by BP86) is about 0.1 Å shorter; the CO bridged Fe–Fe distance (2.705 Å by B3LYP or 2.689 Å by BP86) is about 0.2 Å shorter; and the other three Fe–Fe distances are about 0.1 or 0.2 Å shorter. All of these Fe–Fe distances can be interpreted as the formal single bonds necessary to give all four iron atoms in $Fe_4(CO)_{15}$ the favored 18-electron configuration.

Structure **15-2** (C_{2v} symmetry) lies only ~1 kcal mol^{-1} (B3LYP) or ~2 kcal mol^{-1} (BP86) in energy above the global minimum **15-1**. The B3LYP method predicts for **15-2** a structure with all terminal CO groups with a small imaginary vibrational frequency at 33*i* cm^{-1}. Following the corresponding normal mode leads to **15-1**. The BP86 method predicts a somewhat different **15-2** structure with semibridging carbonyl groups from Fe1 to both Fe2 and the symmetry related Fe3. These semibridging CO groups increase the symmetry

Table 3 The total energies (E, in Hartree), relative energies (ΔE, in kcal mol^{-1}), the zero-point corrected relative energies (ΔE(ZPE), in kcal mol^{-1}), and the numbers of imaginary vibrational frequencies (Nimag) for the structures of $Fe_4(CO)_{15}$

	15-1 (C_s)		**15-2** (C_{2v})	
Method	B3LYP	BP86	B3LYP	BP86
$-E$	6755.47843	6756.50334	6755.47676	6756.49995
ΔE	0	0	1.0	2.1
ΔE(ZPE)	0	0	1.1	2.2
Nimag	0	1 (22i)	1 (33i)	0

equivalent Fe1–Fe2 and Fe1–Fe3 distances to 2.670 Å (B3LYP) or 2.774 Å (BP86). The other two Fe–Fe distances in the four-membered ring are predicted to be 2.931 Å by B3LYP but only 2.696 Å by BP86. The diagonal Fe1–Fe4 distance is predicted to be 2.859 Å (B3LYP) or 2.887 Å (BP86), which is similar to that in **15-1**.

3.3 $Fe_4(CO)_{14}$

Three low-lying singlet structures of $Fe_4(CO)_{14}$ were found (Fig. 4, Table 5 and Table 6). The global minimum **14-1** (D_{2d} symmetry) has a distorted tetrahedral Fe_4 framework with two bridging carbonyls (Fig. 4 and Table 5). The other twelve CO groups are all terminal, with three bonded to each Fe atom. The bridging carbonyl groups exhibit ν(CO) frequencies at 1888 and 1892 cm^{-1} (Table 6), which are >50 cm^{-1} below the terminal ν(CO) frequencies in accord with expectation. The BP86 method predicts all real vibrational frequencies for **14-1** indicating a genuine minimum. The B3LYP method predicts two degenerate small imaginary vibrational frequencies (both 44i cm^{-1}). However, the corresponding B3LYP minima (C_2 and C_s) are very close to the D_{2d} structure with their energies only 0.1 kcal mol^{-1} lower than the D_{2d} structure. The six Fe–Fe bonds in the tetrahedral skeleton are all in the range of 2.620 to 2.664 Å (B3LYP) or 2.608 to 2.610 Å (BP86) corresponding to the single bonds required to give all four iron atoms the favored 18-electron configuration.

The C_s structure **14-2** of $Fe_4(CO)_{14}$ with a central planar Fe_4 butterfly lies 1.5 kcal mol^{-1} lower (B3LYP) or 8.6 kcal mol^{-1} higher (BP86) in energy relative to the global minimum **14-1** with no imaginary vibrational frequencies by either method (Fig. 4 and Table 5). The edge between Fe3 and Fe4 in **14-2** is bridged by two carbonyl groups. These two bridging carbonyl groups are predicted to exhibit ν(CO) frequencies at 1841 and 1857 cm^{-1} (Table 6), which are >100 cm^{-1} lower than the ν(CO) frequencies of the terminal carbonyl groups in accord with expectation. The remaining carbonyl groups in **14-2** are all terminal carbonyl groups, which are asymmetrically located on the Fe atoms with four on Fe1, four on Fe2, three on Fe3, and one on Fe4 (Fig. 4). The Fe2=Fe4 distance in **14-2** is very short, *i.e.*, 2.363 Å (B3LYP) or 2.363 Å (BP86) corresponding to a formal double bond. The Fe3–Fe4 distance is also relatively short, *i.e.*, 2.502 Å (B3LYP) or 2.482 Å (BP86), corresponding to a formal single bond shortened by the two bridging carbonyl groups. The other two Fe–Fe distances of the Fe_4 quadrilateral in the butterfly are relatively long at 2.918 and 3.047 Å (B3LYP) or 2.889 and 2.971 Å (BP86). The diagonal Fe1–Fe4 distance in **14-2** (the body of the butterfly) is predicted to be 2.786 Å (B3LYP) or 2.720 Å (BP86). The one Fe=Fe double bond and the four Fe–Fe single bonds give all four iron atoms in **14-2** the favored 18-electron configuration. No analogous low-energy structure was found for $Os_4(CO)_{14}$ in the previous DFT study.[9]

Table 4 The infrared ν(CO) vibrational frequencies (cm^{-1}) predicted for the four $Fe_4(CO)_{15}$ structures (infrared intensities in parentheses are in km mol^{-1}, semibridging ν(CO) frequencies in **bold**)

15-1	**1854(443)**, **1896(395)**, 1956(2), 1964(13), 1981(90), 1983(6), 1984(134), 1992(265) 1995(33), 2003(16), 2014(2816), 2019(267), 2024(1938), 2041(2248), 2084(39)
15-2	**1876(124)**, **1876(465)**,1963(13), 1967(17), 1967(79), 1976(235), 1984(0), 1989(120), 1991(686), 2006(167), 2015(23), 2016(2812), 2034(1949), 2036(2321), 2085(1)

Table 5 The total energies (E, in Hartree), relative energies (ΔE, in kcal mol^{-1}), the zero-point corrected relative energies (ΔE(ZPE), in kcal mol^{-1}), and the numbers of imaginary vibrational frequencies (Nimag) for the structures of $Fe_4(CO)_{14}$

14	**14-1** (D_{2d})		**14-2** (C_s)		**14-3** (C_{2v})	
Method	B3LYP	BP86	B3LY	PBP86	B3LY	PBP86
$-E$	6642.13278	6643.16794	6642.13522	6643.15470	6642.12040	6643.15410
ΔE	0	0	−1.5	8.6	7.8	9.0
ΔE(ZPE)	0	0	−0.9	8.9	6.3	9.5
Nimag	2 (44i,44i)	0	0	0	1 (29i)	1 (31i)

Table 6 The infrared ν(CO) vibrational frequencies (cm^{-1}) predicted for the three $Fe_4(CO)_{14}$ structures (infrared intensities in parentheses are in km mol^{-1}, bridging ν(CO) frequencies in **bold**)

14-1	**1888(0)**, **1892(792)**, 1947(94), 1947(94), 1950(0), 1950(154), 1991(0), 2000(0), 2003(466), 2003(466), 2026(1917), 2028(2119), 2028(2119), 2071(0)
14-2	**1841(340)**, **1857(89)**, 1967(195), 1976(273), 1983(58), 1987(14), 1994(132), 1995(235), 2006(96), 2013(741), 2014(1830), 2032(1294), 2041(2584), 2079(79)
14-3	**1876(0)**, **1896(998)**, **1900(144)**, **1920(135)**, 1974(0), 1981(45), 1988(3) 1995(43), 2000(31), 2016(318), 2022(2502), 2034(1840), 2040(2017), 2076(48)

The C_{2v} structure **14-3** of $Fe_4(CO)_{14}$ has a tetrahedral arrangement of the iron atoms (Fig. 4, Table 5 and Table 6) and lies in energy above **14-1** by 7.8 kcal mol^{-1} (B3LYP) or 9.0 kcal mol^{-1} (BP86). Structure **14-3** has one imaginary vibrational frequency at $29i$ cm^{-1} (B3LYP) or $31i$ cm^{-1} (BP86). Following the corresponding normal mode leads to the global minimum **14-1**.

3.4 Dissociation energies

The dissociation energies are obtained from the difference between the total energies of the dissociation products and that of the original complex. Table 7 summarizes the energies for different dissociation pathways for the global minima of $Fe_4(CO)_n$ (n = 16, 15, 14). These data were obtained by using total energies calculated by the same methods for the dissociation fragments $Fe_3(CO)_n$ (n = 12, 11, 10, 9), $Fe_2(CO)_n$ (n = 9, 8, 7), $Fe(CO)_n$ (n = 5, 4), and CO; the results are in essential agreement with those given in the literature.[30,31] When one of the dissociation fragments of the tetranuclear iron carbonyl is the stable molecule $Fe(CO)_5$ or $Fe_3(CO)_{12}$, the dissociation is predicted to require relatively little energy. For example, the dissociation of $Fe_4(CO)_{16}$ into $Fe(CO)_5$ + $Fe_3(CO)_{11}$ is predicted to require only 1.9 kcal mol^{-1} (B3LYP) or 0.1 kcal mol^{-1} (BP86) and thus to be essentially thermoneutral. The alternative dissociation pathway of $Fe_4(CO)_{16}$ into $Fe_3(CO)_{12}$ + $Fe(CO)_4$ is also predicted to require relatively little energy at 1.5 kcal mol^{-1} (B3LYP) or 5.8 kcal mol^{-1} (BP86). The predicted low dissociation energies of $Fe_4(CO)_{16}$ by either of these pathways suggest this to be an unstable molecule consistent with the fact that it has never been synthesized or even detected spectroscopically in low temperature matrices.

A similar dissociation of $Fe_4(CO)_{15}$ into $Fe(CO)_5$ + $Fe_3(CO)_{10}$ is predicted to require only 3.3 kcal mol^{-1} (B3LYP) or 6.2 kcal mol^{-1} (BP86). This suggests that $Fe_4(CO)_{15}$, like $Fe_4(CO)_{16}$, is a relatively unstable molecule consistent with the fact that it has never been synthesized. The carbonyl dissociation energy of $Fe_4(CO)_{15}$ to $Fe_4(CO)_{14}$ + CO is also relatively low at 10.6 kcal mol^{-1} (B3LYP) or 4.8 kcal mol^{-1} (BP86) suggesting the facile conversion of $Fe_4(CO)_{15}$ into $Fe_4(CO)_{14}$.

The thermodynamics summarized in Table 7 suggests that $Fe_4(CO)_{14}$ could be stable enough to be a detectable molecule consistent with its detection from the reaction of mass-selected Fe_4^+ with carbon monoxide in low-temperature matrices.[5] Thus the dissociation of $Fe_4(CO)_{14}$ into $Fe(CO)_5$ + $Fe_3(CO)_9$ is predicted to require the relatively large energy of 23.2 kcal mol^{-1} (B3LYP) or 39.2 kcal mol^{-1} (BP86). The alternative dissociation pathway of $Fe_4(CO)_{14}$ into $Fe(CO)_4$ + $Fe_3(CO)_{10}$, which does not give one of the stable iron carbonyls $Fe(CO)_5$, $Fe_2(CO)_9$, or $Fe_3(CO)_{12}$, requires even more energy at 35.1 kcal mol^{-1} (B3LYP) or 51.2 kcal mol^{-1} (BP86). This, as well as the relatively low carbonyl dissociation energy of $Fe_4(CO)_{15}$ into $Fe_4(CO)_{14}$ + CO noted above, suggests the viability of $Fe_4(CO)_{14}$ as a potentially synthesizable molecule. Possibly an oxidative carbonylation of the known[6,7] $Fe_4(CO)_{13}{}^{2-}$ under sufficiently mild conditions might provide a route to $Fe_4(CO)_{14}$.

Table 7 Dissociation energies (kcal mol^{-1}) for $Fe_4(CO)_n$ (n = 16, 15, 14) based on the lowest energy structures. The zero point energy corrected dissociation energies are given in parentheses

	B3LYP	BP86
$Fe_4(CO)_{16} \rightarrow Fe_4(CO)_{15} + CO$	22.4 (20.3)	25.3 (23.0)
$Fe_4(CO)_{16} \rightarrow 2\ Fe_2(CO)_8$	12.1 (10.0)	4.1 (2.1)
$Fe_4(CO)_{16} \rightarrow Fe(CO)_5 + Fe_3(CO)_{11}$	1.9 (0.2)	0.1 (−1.7)
$Fe_4(CO)_{16} \rightarrow Fe(CO)_4 + Fe_3(CO)_{12}$	1.5 (0.2)	5.8 (4.3)
$Fe_4(CO)_{15} \rightarrow Fe_4(CO)_{14} + CO$	10.6 (7.7)	4.8 (2.4)
$Fe_4(CO)_{15} \rightarrow Fe_2(CO)_8 + Fe_2(CO)_7$	15.0 (12.5)	17.4 (15.2)
$Fe_4(CO)_{15} \rightarrow Fe(CO)_4 + Fe_3(CO)_{11}$	21.9 (19.5)	24.4 (22.4)
$Fe_4(CO)_{15} \rightarrow Fe(CO)_5 + Fe_3(CO)_{10}$	3.3 (1.0)	6.2 (4.2)
$Fe_4(CO)_{14} \rightarrow Fe_4(CO)_{13} + CO$	27.5 (25.5)	33.4 (31.0)
$Fe_4(CO)_{14} \rightarrow 2\ Fe_2(CO)_7$	29.6 (27.6)	51.2 (48.8)
$Fe_4(CO)_{14} \rightarrow Fe(CO)_4 + Fe_3(CO)_{10}$	35.1 (32.8)	51.2 (48.8)
$Fe_4(CO)_{14} \rightarrow Fe(CO)_5 + Fe_3(CO)_9$	23.2 (22.2)	39.2 (37.9)

Another indication that $Fe_4(CO)_{14}$ might be a viable molecule is suggested by the studies by Fedrigo, Haslett, and Moskovits (FHM)[5] of the codeposition of mass-selected Fe_4^+ with carbon monoxide at 25 K followed by neutralization of the resulting ions with an electron beam. The resulting infrared spectrum in the ν(CO) region, although broad, complicated, and poorly resolved, shows a feature at 1889 cm^{-1} that could correspond to the predicted infrared-active bridging ν(CO) frequency at 1892 cm^{-1} for the $Fe_4(CO)_{14}$ structure **14-1** (Table 6). The quality of the remainder of the spectrum is too poor to compare in detail with our predicted ν(CO) frequencies. In any case, our DFT studies on $Fe_4(CO)_{14}$ are consistent with the FHM claim of the generation of $Fe_4(CO)_{14}$ in low-temperature matrices. Clearly more work on this system is needed.

4. Summary

The structures predicted for the tetranuclear iron carbonyls $Fe_4(CO)_n$ (n = 16, 15, 14) are seen in many respects to be analogous to those of the known osmium compounds, which are stable enough for isolation and structure determination by X-ray crystallography. Thus, low-energy structures are predicted for $Fe_4(CO)_{16}$, $Fe_4(CO)_{15}$, and $Fe_4(CO)_{14}$ in which the Fe_4 units are rhombi, planar butterflies, and tetrahedral with the four, five, and six Fe–Fe single bonds, respectively, required to give all four iron atoms the favored 18-electron configuration. However, for $Fe_4(CO)_{14}$ an alternative low energy structure is predicted with a planar Fe_4 butterfly and one of the five iron–iron distances short enough to correspond to a formal Fe═Fe double bond, thereby also leading to the favored 18-electron configuration for all four iron atoms. An analogous structure has not been found for $Os_4(CO)_{14}$ either as a stable compound or a low-energy structure predicted by density functional theory.[9]

An interesting aspect of the chemistry of iron carbonyls is the fact that none of the tetranuclear iron carbonyls $Fe_4(CO)_n$ (n = 16, 15, 14) are known as stable molecules unlike their osmium analogues. In this connection, the dissociation energies of $Fe_4(CO)_{16}$ into $Fe(CO)_5$ + $Fe_3(CO)_{11}$ or $Fe_3(CO)_{12}$ + $Fe(CO)_4$ are predicted to be very low (<6 kcal mol^{-1}). Similarly, the dissociation energy of $Fe_4(CO)_{15}$ into $Fe(CO)_5$ + $Fe_3(CO)_{10}$ is predicted to be very low at ~5 kcal mol^{-1}. These low predicted dissociation energies of $Fe_4(CO)_{16}$ and $Fe_4(CO)_{15}$ into smaller iron carbonyl fragments are consistent with the fact that neither of these molecules have been synthesized or even detected spectroscopically in low temperature matrices. However, $Fe_4(CO)_{14}$ is predicted to be considerably more stable towards dissociation into smaller fragments with a dissociation energy of 23 kcal mol^{-1} (B3LYP) or 39 kcal mol^{-1} (BP86) into $Fe(CO)_5$ + $Fe_3(CO)_9$. This is consistent with the detection of $Fe_4(CO)_{14}$ by infrared spectroscopy in the reaction product of mass selected Fe_4^+ with CO in low temperature matrices.[5]

Acknowledgements

We are indebted to the 111 Project (B07012) in China and the US National Science Foundation (Grants CHE-0749868 and CHE-0716718) for support of this research.

References

1 V. J. Johnston, F. W. B. Einstein and R. K. Pomeroy, *J. Am. Chem. Soc.*, 1987, **109**, 8111.
2 F. W. B. Einstein, V. J. Johnston and R. K. Pomeroy, *Organometallics*, 1990, **9**, 2754.
3 V. J. Johnston, F. W. B. Einstein and R. K. Pomeroy, *J. Am. Chem. Soc.*, 1987, **109**, 7220.
4 V. J. Johnston, F. W. B. Einstein and R. K. Pomeroy, *Organometallics*, 1988, **7**, 1867.
5 S. Fedrigo, T. L. Haslett and M. Moskovits, *Chem. Phys. Lett.*, 1999, **307**, 333.
6 W. Hieber, F. Sonnekalb and E. Becker, *Chem. Ber.*, 1930, **63**, 973.
7 R. J. Doedens and L. F. Dahl, *J. Am. Chem. Soc.*, 1966, **88**, 4847.
8 C. Corminboeuf, P. v. R. Schleyer and R. B. King, *Chem.–Eur. J.*, 2007, **13**, 978.
9 B. Xu, Q.-S. Li, Y. Xie, R. B. King and H. F. Schaefer, *Dalton Trans.*, 2008, 1366.
10 A. W. Ehlers and G. Frenking, *J. Am. Chem. Soc.*, 1994, **116**, 1514.
11 B. Delley, M. Wrinn and H. P. Lüthi, *J. Chem. Phys.*, 1994, **100**, 5785.
12 J. Li, G. Schreckenbach and T. Ziegler, *J. Am. Chem. Soc.*, 1995, **117**, 486.
13 V. Jonas and W. Thiel, *J. Chem. Phys.*, 1995, **102**, 8474.
14 T. A. Barckholtz and B. E. Bursten, *J. Am. Chem. Soc.*, 1998, **120**, 1926.
15 S. Niu and M. B. Hall, *Chem. Rev.*, 2000, **100**, 353.
16 P. Macchi and A. Sironi, *Coord. Chem. Rev.*, 2003, **238–239**, 383.
17 J.-L. Carreón-Macedo and J. N. Harvey, *Phys. Chem. Chem. Phys.*, 2006, **8**, 93.
18 M. Bühl and H. Kabrede, *J. Chem. Theory Comput.*, 2006, **2**, 1282.
19 A. D. Becke, *J. Chem. Phys.*, 1993, **98**, 5648.
20 C. Lee, W. Yang and R. G. Parr, *Phys. Rev. B: Condens. Matter*, 1988, **37**, 785.
21 A. D. Becke, *Phys. Rev. A: At., Mol., Opt. Phys.*, 1988, **38**, 3098.
22 J. P. Perdew, *Phys. Rev. B: Condens. Matter*, 1986, **33**, 8822.
23 T. H. Dunning, *J. Chem. Phys.*, 1970, **53**, 2823.
24 S. Huzinaga, *J. Chem. Phys.*, 1965, **42**, 1293.
25 A. J. H. Wachters, *J. Chem. Phys.*, 1970, **52**, 1033.
26 D. M. Hood, R. M. Pitzer and H. F. Schaefer, *J. Chem. Phys.*, 1979, **71**, 705.
27 M. J. Frisch *et al.*, *GAUSSIAN 03, Revision C 02*, Gaussian, Inc., Wallingford CT, 2004 (see ESI for details).
28 C. H. Wei and L. F. Dahl, *J. Am. Chem. Soc.*, 1966, **88**, 1821.
29 F. A. Cotton and J. M. Troup, *J. Am. Chem. Soc.*, 1974, **96**, 4155.
30 H. Wang, Y. Xie, R. B. King and H. F. Schaefer, III, *J. Am. Chem. Soc.*, 2006, **128**, 11376.
31 J. Jang, J. Lee and H. Lee, *J. Phys. Chem. A*, 1998, **102**, 5298.